High Current Efficiency and Low Temperature Characteristic of Organic Materials

Chih-I Wu (吳志毅)^{1,2}, Chang-Ting Lin (林昌廷)², Yu-Hung Chen (陳裕宏)², Mei-Hsin Chen (陳美杏)², Jheng-Hao Fang (方正豪)², and Guan-Ru Lee (李冠儒)²

¹Department of Electrical Engineering, National Taiwan University, Taipei, Taiwan ²Graduate Institute of Electro-optical Engineering, National Taiwan University, Taipei, Taiwan

A highly efficient hole injection material, boron subphthalocyanine chloride (SubPc), was incorporated in organic light-emitting diodes. Device performance is greatly enhanced by inserting an ultrathin layer of SubPc between anodes and N,N'-di(naphthalene-1-yl)-N,N'diphenyl-benzidene (NPB). Electronic structures and chemical reaction at the interface between NPB and SubPc also investigated by photoemission are spectroscopy with synchrotron radiation sources. Extra states are observed at the forbidden gap of SubPc with deposition of NPB, resulting from the broken bonds between boron and chlorine on SubPc with presence of NPB. These gap states are attributed to the improvement of device performance.

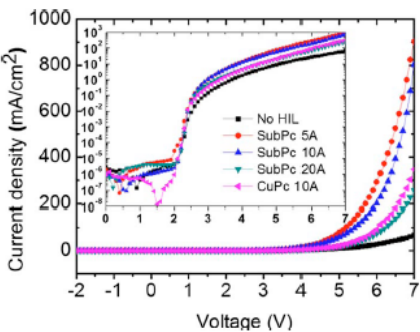


Fig. 1: Current density-voltage (*J-V*) characteristics of OLEDs with different HILs.

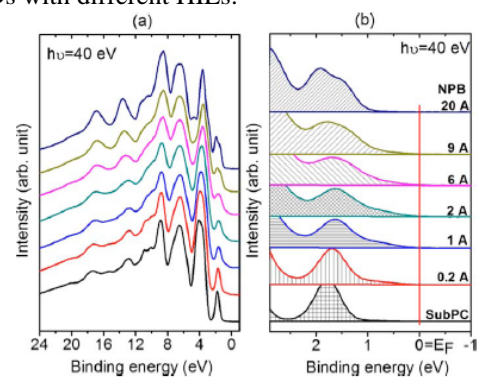


Fig. 2: (a) Valence band spectra of SubPc with incremental deposition of NPB. (b) Valence band spectra close to the Fermi level.

Influences of temperature and intramolecular interaction on the electronic structures of oligofluorenes were systematically studied via synchrotron radiation photoemission spectroscopy and quantum chemical calculations. Our results show that the oligofluorene thin films deposited at substrates of different temperatures

will alter the electronic structures, which results from the change of interunit angles in 2,7-bis[9,9-di(4-methylphenyl)-fluoren-2-yl]-9,9-di(4-methylphenyl) fluorine molecules. The fluorene-units at low temperature are almost perpendicular to each other and the interunit angle of stable state is 41° at room temperature.



Fig. 3: The chemical structures of TDAF.

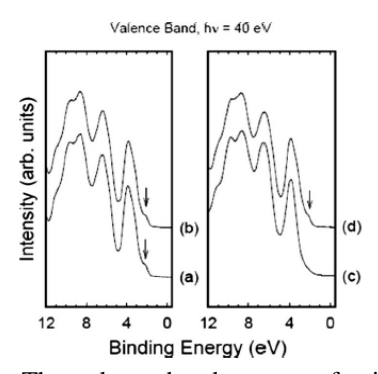


Fig. 4: The valence band spectra of pristine TDAF for different evaporation/measurement conditions, (a) RT/RT, (b) RT/LT, (c) LT/LT, and (d) LT/RT. Only the spectrum (c) shows different features at the top of HOMO.

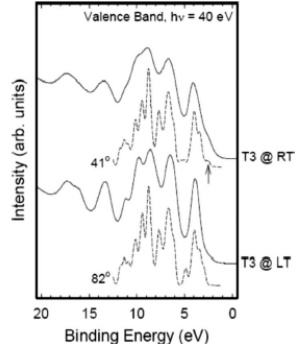


Fig. 5: The comparison of experimental and theoretical valence band spectra of TDAF.